

ELECTRON TRANSPORT THROUGH A QUANTUM CAVITY

Y. Wang, W. Y. Deng, and S. Y. Chou
 Department of Electrical Engineering, University of Minnesota
 Minneapolis, MN 55455, U. S. A.

(Received 10 January 1995)

Electron transport through a quantum cavity coupled with two one-dimensional waveguides is studied using a generalized scattering matrix method. In a symmetric N -channel cavity model, we are able to obtain an exact solution that predicts the electron energies at which the transmission of electron waves become zero. We found that the zero of transmission is closely related to the longitudinal resonance through inter-channel scattering, in particular, to the resonance of the highest propagating mode inside the cavity. This model provides a simple way to calculate the electron transmission through a cavity which could be useful in quantum waveguide engineering.

1. Introduction

Electron transport through coupled quantum waveguides show interesting interference patterns.¹ Previously, various types of waveguide structures, such as a cavity,²⁻⁴ T-shape stub⁵⁻⁷ or double bend,² were investigated, mostly by computer simulations. Here, we perform an analytical study of the electron transmission through a quantum cavity coupled with two one-dimensional waveguides using a generalized scattering matrix method. In a symmetric N -channel cavity model, we are able to obtain an exact solution that predicts the electron energies at which the transmission of electron waves become zero. We will show that the zero transmission is closely related to the longitudinal resonance and inter-mode scattering inside the cavity. The model provides a simple way to calculate the electron transmission through a cavity which could be useful in quantum waveguide engineering.

2. Model

To establish the model, let us consider a rectangular cavity coupled to two identical one-dimensional (1D) waveguides (leads) as depicted in Fig. 1(a). We make three simplifications. First, we adopt the standard hard wall approximation, thus the threshold energy of each lateral mode is simply $\epsilon_n^{(i)} \approx \hbar^2/2m^* (\pi n/w_i)^2$, where m^* is the

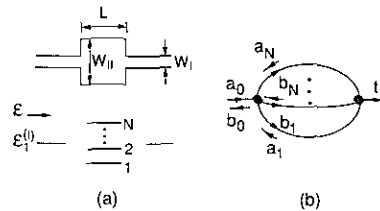


Fig. 1 (a) A rectangular cavity coupled to two identical 1D leads. Only one propagating mode exists in the leads, but there are N propagating modes inside the cavity. (b) In this model, all evanescent waves are neglected, therefore the cavity is equivalent to N thin wires joined together at two ends.

effective mass of an electron, n is the mode index, w_i is the width in the i th region, and $i = I, II$ denotes the leads and the cavity, respectively. Second, we neglect all the evanescent waves in the cavity which decay exponentially with the cavity length, L . In exact numerical calculations, the evanescent waves are necessary since they contribute significantly to the boundary matching. But in our S-matrix treatment, the effects of the evanescent waves can be largely taken into account by a rescaling of the matrix elements.⁸

Finally, since the zero transmission occurs only when the incoming electron energy, ϵ , is between $\epsilon_1^{(I)}$ and $\epsilon_2^{(I)}$, we only need to consider one propagation mode in the leads. Inside the cavity, we will consider N even-parity propagation modes with N determined by $\epsilon_{(2N-1)}^{(II)} < \epsilon < \epsilon_{(2N+1)}^{(II)}$. Because the incident electron wave has an even parity, it does not couple to any odd-parity mode in the cavity, due to parity conservation.

In this model, the cavity is equivalent to N thin wires with each wire containing only one propagating mode (channel), and the wave-vector in the i th channel is given by $\beta_i = [\epsilon - \epsilon_{(2i-1)}^{(II)}]^{1/2}$. The model can be easily generalized to an asymmetric cavity.

3. Results

The electron transport through the cavity is determined by the scattering at the two junctions as well as the propagation inside the cavity. The scattering at each junction can be described by a generalized S-matrix. For a symmetric N -channel cavity described above, the two junctions have the same S-matrix defined by $S_{ij} = (b_i/a_j)_{a_k=0, k \neq j}$, where a_i and b_i are the normalized amplitudes of incoming and outgoing waves in the i th channel ($i = 0, 1, \dots, N$), the index 0 denotes the first mode in the leads. S_{ij} is related to the conventional transmission coefficient, t_{ij} , by $S_{ij} = \sqrt{\beta_i/\beta_j} t_{ij}$. It can be shown that the transmission from the left to the right leads is given by⁹

$$t = [s_{0i}] P (I - [S]_N P [S]_N P)^{-1} [s_{i0}] \quad (1)$$

where I is the identity matrix, $[S]_N$ is the S-matrix without first row and first column, $[s_{i0}] = (S_{10}, \dots, S_{N0})^T$, $[s_{0i}] = (S_{01}, \dots, S_{0N})$, and P is the propagation matrix, defined by $P_{ij} = e^{i\theta_i} \delta_{ij}$ with $\theta_i = \beta_i L$ which denotes the phase delay in the i th channel. The physical meaning of Eq. (1) is quite clear. $[s_{i0}]$ ($[s_{0i}]$) represents the coupling between the incoming (outgoing) lead and the cavity. The inverse matrix describes the multiple reflections within the cavity. Notice that Eq. (1) has exactly the same form as that in a 1D Fabry-Perot resonator, except the phase delay and internal reflection coefficients are now described by matrices because of the multiple channels in the cavity.

3.1 Two Channels in a Cavity

Since in our model only propagating waves are involved, the S-matrix must be real. The current conservation and time reversal invariance require the S-matrix to be unitary and symmetric.¹⁰ A simple way to construct such a unitary symmetric matrix is only using the coupling coefficients $[s_{i0}]$, we have:

$$\begin{aligned} S_{ii} &= 1 - S_{i0}^2 / (1 - S_{00}) \\ S_{ij} &= -S_{i0} S_{j0} / (1 - S_{00}) \quad (i, j = 1, \dots, N) \end{aligned} \quad (2)$$

For $N = 2$, the above expression is a general solution, and a simple form of transmission coefficient can be obtained:

$$t = C/D \quad (3)$$

where

$$C = S_{10}^2 e^{i\theta_1} f_2 + S_{20}^2 e^{i\theta_2} f_1 \quad (3a)$$

$$D = \{1 - S_{00} e^{i(\theta_1 + \theta_2)}\}^2 - \{S_{11} e^{i\theta_1} + S_{22} e^{i\theta_2}\}^2 \quad (3b)$$

and $f_j = 1 - e^{i2\theta_j}$, $j = 1, 2$. The result can also be applied to a ring structure, which was previously studied by Gefen *et al.*¹⁰ in the context of Aharonov-Bohm interference effect.

From Eq. (3a), we find the zero transmission occurs when $\sin\theta_2/\sin\theta_1 = -(S_{20}/S_{10})^2$. The solution of this equation is quite insensitive to the precise choice of S_{20}/S_{10} . To get quantitative results, we use a simple 1D approximation for S_{10} and S_{20} :

$$S_{i0} = -\frac{2\sqrt{\alpha\beta_i}}{(\alpha + \beta_i)} \langle \alpha | \beta_i \rangle \quad (4)$$

where α is the wave-vector in the leads, β_i is the wave-vector of the i th channel in the cavity, and $\langle \alpha | \beta_i \rangle$ is the overlap integral between the lateral wave functions of the first mode in the leads and the i th mode in the cavity. The transmission probability calculated from Eqs. (3) and (4) is shown in Fig. 2(a). The exact numerical result calculated using mode-matching technique² is plotted in Fig. 2(b).

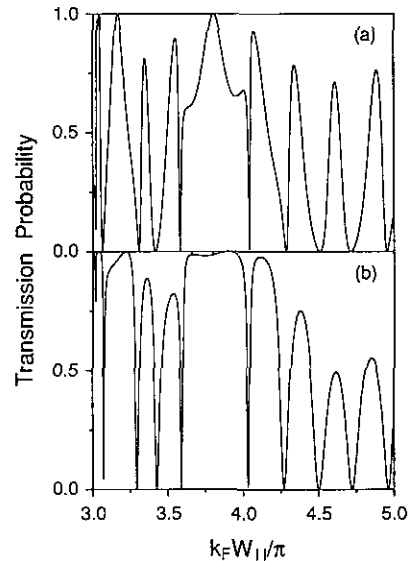


Fig. 2 (a) Transmission probability calculated from Eqs. (3) and (4); (b) exact numerical result calculated using mode-matching technique. k_F is the Fermi wavelength of the incident electron. The dimensions of the cavity are: $W_I = 10$ nm, $W_{II} = 25$ nm, and $L = 75$ nm.

The general shapes of the two curves agree with each other. In particular, the zero transmission points coincide almost exactly. This shows that the simple model not only gives a qualitatively correct description, but also provides an easy way to determine the zero transmission points.

3.2 Multiple Channels in a Cavity

For an N -channel cavity with $N > 2$, in general, $[S_{i0}]$ is not sufficient to determine the entire S -matrix. However, to gain physical insights, we may still use Eq. (2) to construct $[S]_N$. Later, we will compare the results with the exact numerical calculations. Similar to the two-channel case [Eq. (3a)], we obtain:

$$C = \sum_{i=1}^N S_{i0}^2 e^{i\theta_i} \prod_{j \neq i} f_j \quad (5)$$

Notice that, in Eq. (5), there are no off-diagonal terms ($S_{i0}S_{j0}$, $j \neq i$). This stems from the unitary property of the S -matrix, which allows all the off-diagonal terms in Eq. (2) to be combined into diagonal terms.

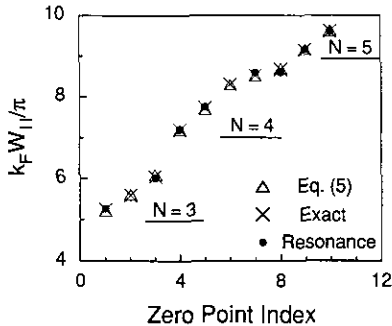


Fig. 3 The position of zero transmission calculated for $N = 3, 4, 5$. Δ : using Eq. (5), \times : exact numerical result, \bullet : from resonance condition of the highest propagating mode, i.e., $\theta_N = m\pi$. The dimensions of the cavity are: $W_I = 10$ nm, $W_{II} = 50$ nm, and $L = 30$ nm.

Figure 3 shows the zero transmission points calculated from Eq. (5) for $N = 3, 4, 5$, respectively. The agreement with the values calculated using mode-matching technique is excellent. Surprisingly, we found most of the zeros occur near the resonance of the highest propagating mode, as indicated by the solid circle in Fig. 3. This interesting result can be illuminated by examine Eq. (5). From Eq. (5), we observe that each propagating channel inside the cavity affects the other propagating channels through a factor $f_j = 1 - e^{i2\theta_j}$. If the i th channel is in longitudinal

resonance, all the terms but the i th term in the summation of Eq. (5) vanish. This suggests that a zero transmission is most probable to occur near a longitudinal resonant energy. Since the highest propagating mode (channel N) has the smallest wave-vector, its phase changes fastest as the electron energy changes ($\Delta\theta \propto \Delta\beta \propto \Delta\epsilon/\beta$). This means the highest propagating mode has more longitudinal resonance in a given energy range than those lower modes. Thus, the zero transmission is more likely to occur near the resonance of the highest propagating mode.

To see the importance of the mode mixing inside the cavity to the zero transmission, we set all the off-diagonal matrix elements of $[S]_N$ to zero so that there is no inter-channel scattering. Then Eq. (2) reduces to:

$$t = \sum_{i=1}^N t_i \quad (6)$$

where

$$t_i = S_{i0}^2 \frac{e^{i\theta_i}}{1 - S_{ii}^2 e^{i2\theta_i}} \quad (6a)$$

As expected, each channel propagates independently, and the total transmission is simply the coherent sum of the transmissions from all channels. If we further use Eq. (4) for S_{i0} and set $S_{ii} = (\beta_i - \alpha)/(\beta_i + \alpha)$, t_i becomes exactly the transmission through a 1D potential well but weighted by a factor $\langle \alpha | \beta_i \rangle^2$. The transmission coefficient thus calculated is shown in Fig. 4. It shows that, without inter-channel scattering, all the sharp oscillations and zero transmission disappear, only the envelope is preserved. This means the mode mixing is essential to the zero transmission.

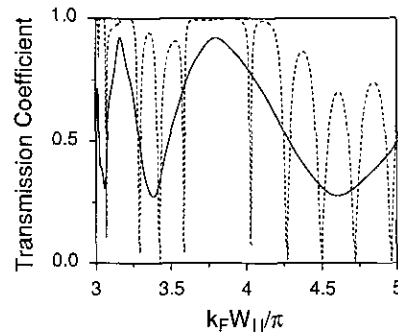


Fig. 4 Amplitude of transmission coefficient calculated using Eq. (6), it can be regarded as an average of the exact solution (dashed line). The cavity dimensions are the same as in Fig. 2.

So far, our discussions are limited to zero temperature. At finite temperature T , the incident electrons are no longer monochromatic but have an energy smearing on the order of kT around the Fermi energy. It is easy to show that the transmission at finite T is simply a convolution of the transmission at zero temperature and the derivative of a Fermi-Dirac distribution function. Since the convolution is essentially a weighted average process, the transmission curve at finite T will look like a smoothing of the transmission curve at zero temperature. As a result, the sharp oscillations will diminish and the transmission minima will have a finite value instead of zero. These effects have been observed in our recent experiment.¹¹

4. Summary

In summary, we have established an analytically solvable model which allows us to determine the electron zero transmission points through a cavity. We have shown that the zero transmission is closely related to the longitudinal resonance inside the cavity, especially the resonance of the highest propagating mode. Furthermore, the inter-channel scattering must be included in order to understand zero transmission. This model provides a simple way to calculate the electron transmission through a cavity which could be useful in quantum waveguide engineering.

Acknowledgment--This work is partially supported by ONR, ARPA, and ARO.

5. References

¹See, for example, "Nanostructure Physics and Fabrication", Edited by M. A. Reed and W. P. Kirk, Academic Press, San Diego, 1990.

²A. Weisshaar, J. Lary, S. M. Goodnick, and V. K. Tripathi, Appl. Phys. Lett. **55**, 2114 (1989); see also, A. Weisshaar, J. Lary, S. M. Goodnick, and V. K. Tripathi, J. Appl. Phys. **70**, 355 (1991).

³C. S. Lent and S. Sivaprakasam, in "Nanostructures and Microstructure Correlation with Physical Properties of Semiconductors", edited by H. G. Craighead and J. M. Gibson, SPIE proceedings, San Diego, California, March, 1990.

⁴F. M. Peeters, in "Science and Engineering of One- and Zero-Dimensional Semiconductors", edited by S. P. Beaumont and C. M. S. Torres, Plenum Press, New York, 1990.

⁵F. Sols, M. Macucci, U. Ravaoli, and K. Hess, Appl. Phys. Lett. **54**, 350 (1989).

⁶D. F. Berggren and Z. Ji, Superlattices and Microstructures, **8**, 59 (1990).

⁷S. Datta, Superlattices and Microstructures, **6**, 83 (1989).

⁸For the extreme case of a single δ -function scatterer in a wire, it has been shown before that the total effect of the evanescent modes is to rescale the mode coupling constants of the propagating modes. See P. F. Bagwell, Phys. Rev. **B41**, 10354 (1990). For a cavity in a wire, this does not hold in general, but we found it still a good approximation except near the onset of a new mode where the decaying constant approaches to zero.

⁹Y. Wang, W. Y. Deng, and S. Y. Chou, unpublished.

¹⁰Y. Gefen, Y. Imry, and M. Y. Azbel, Phys. Rev. Lett. **52**, 129 (1984).

¹¹Y. Wang and S. Y. Chou, Appl. Phys. Lett. **65** (16), 1994.